Vol. 25, No. 1(2026) Mat26686

Revista Mexicana de Ingeniería Química

Towards low-carbon cement: evaluating ferrochrome and steel slags as supplementary cementitious materials

Hacia un cemento bajo en carbono: evaluación de escorias de ferrocromo y de acero como materiales cementantes suplementarios

M. Hoxhaj*, S. Vishkulli, I. Boci, S. Vito, Xh. Hyseni

Department of Industrial Chemistry, Faculty of Natural Sciences, University of Tirana, Blv. Zogu I, 1001, Tirana, Albania.

Received: September 29, 2025; Accepted: December 27, 2025

Abstract

With a growing focus on decarbonizing construction, alternative binders from industrial waste offer sustainable solutions with significant environmental and economic benefits. This study investigates the potential of ferrochrome and steel slags, byproducts of Albania's metallurgical sector, as partial cement replacements. Mortar samples with 30% slag substitution were tested for physical and mechanical properties. At 28 days, the slag mixtures retained 62.3% (black), 68.6% (Fe–Cr), and 87.3% (white) of the reference compressive strength (CEM I 42.5R). Setting times increased compared to the control, with initial setting extending from 110 min (CEM I) to 140-250 min and final setting from 230 min to 250-350 min depending on slag type. Water demand rose from 126ml (CEM I) to 144-189 ml for slag-containing mixes. Despite reduced early strength, white steel slag demonstrated pozzolanic activity indicating potential for cementitious applications, whereas black and Fe-Cr slags showed limited reactivity, suggesting the need for activation or further optimization to improve their performance. Overall, the findings support the technical feasibility of incorporating industrial slags into eco-efficient cement formulations.

Keywords: eco-efficient cement, industrial waste, ferro-chrome slag, steel slag, compressive strength.

Resumen

Con el creciente enfoque en la descarbonización de la construcción, los aglomerantes alternativos derivados de residuos industriales ofrecen soluciones sostenibles con beneficios ambientales y económicos significativos. Este estudio investiga el potencial de las escorias de ferro-cromo y acero, subproductos del sector metalúrgico de Albania, como sustitutos parciales del cemento. Se evaluaron morteros con un 30% de sustitución por escoria, analizando propiedades físicas y mecánicas. A los 28 días, las mezclas con escoria retuvieron el 62.3% (escoria negra), 68.6% (Fe–Cr) y 87.3% (escoria blanca) de la resistencia a compresión del material de referencia (CEM I 42.5R). Los tiempos de fraguado aumentaron en comparación con el control, con el fraguado inicial pasando de 110 min (CEM I) a 140–250 min y el fraguado final de 230 min a 250-350 min, según el tipo de escoria. La demanda de agua aumentó de 126 ml (CEM I) a 144-189 ml en las mezclas con escoria. A pesar de la menor resistencia inicial, la escoria blanca mostró actividad puzolánica, lo que indica potencial para aplicaciones cementicias, mientras que las escorias negra y Fe-Cr presentaron reactividad limitada, lo que sugiere la necesidad de activación u optimización adicional para mejorar su desempeño. En general, los resultados respaldan la viabilidad técnica de incorporar escorias industriales en formulaciones de cemento ecoeficientes.

Palabras clave: cemento ecoeficiente, residuos industriales, escoria de ferrocromo, escoria de acero, resistencia a la compresión.

*Corresponding author. *E-mail*: maria.hoxhaj@fshn.edu.al ;

https://doi.org/10.24275/rmiq/Mat26686

ISSN:1665-2738, *issn-e*: 2395-8472

1 Introduction

Cement production plays a major role in construction, but it's increasingly under pressure due to its environmental impact, especially CO_2 emissions. The production of ordinary Portland cement (OPC) releases CO_2 during the calcination of limestone and is largely dependent on fossil fuels. Because of these dual effect, OPC manufacturing is positioned as a significant contributor to greenhouse gas emissions worldwide (Schneider *et al*., 2011). One promising strategy to mitigate these emissions is the incorporation of supplementary cementitious materials (SCMs) into concrete formulations to partially replace OPC, or directly into cement production to substitute clinker, the most carbon-intensive component of cement (Scrivener *et al*., 2018).

These materials, although mostly by-products of industry or natural occurring minerals, create a double-through environmental advantage: they reduce the carbon footprint of the cement production, and second, they promote materials recycling that otherwise would have contributed to landfills or environmental pollution (Owaid *et al*., 2012). This shift reflects a broader movement toward more sustainable material consumption and ecologically friendly building practices. A wide range of supplementary cementitious materials (SCMs), including naturally occurring pozzolans such as volcanic ash and industrial by-products like fly ash, ground granulated blast furnace slag, silica fume, and metakaolin, are recognized for their role in enhancing sustainability in cement production and similar investigations on alkali-activated and geopolymer systems derived from aluminosilicate industrial by-products have also been reported (Owaid *et al*., 2012; Lothenbach *et al*., 2011, Montañez-Cervantes *et al*., 2024, Torres-Ochoa *et al*., 2019). In recent years, additional waste-derived materials, such as rice husk ash, coal ash, and calcined clays, have been explored as SCMs or precursors in blended-cement and geopolymer systems. Leklou and Das (2023) reported that metakaolin addition enhances binder reactivity and accelerates hydration at high temperatures. Das *et al*. (2020) demonstrated that optimized rice husk ash can improve the sustainability of geopolymer concretes, while Das *et al*. (2021) highlighted coal ash as a viable by-product for producing durable building materials. Tripathi *et al*. (2025) further emphasized the potential of ferrochrome slag for industrial waste reuse. These studies show that the performance of SCMs depends on their reactivity, mineralogy, and processing conditions, positioning the present research on ferrochrome and steel slags within this broader sustainability framework, while highlighting that durability and environmental behavior remain critical considerations for sustainable cementitious systems (Ramírez-Arreola *et al*., 2020).

Instead of being discarded as landfill waste, those materials can be beneficially reused in cement and concrete production. This, offers advantages like lower energy during clinker production, enhanced concrete properties, and a lessened environmental footprint (Scrivener *et al*., 2018). By utilizing what would otherwise be waste, the industry can conserve natural resources, lower emissions, and advance a circular economy model, transforming waste materials into valuable resources (Owaid *et al*., 2012).

Among the various types of industrial residues, ferrochrome and steel slag are produced in significant quantities, particularly in metallurgical regions. Slag is a byproduct obtained from metallurgical processes, particularly during the production of ferroalloys and carbon or stainless steels. It is produced in a blast or electric arc furnace when impurities like silica, alumina, and lime are exposed to high temperatures and go through a fluxing reaction. Following immediate cooling with either water or air this mass solidifies producing granulated or crystalline slag. Steel slag, for instance, is rich in calcium silicates (C_2S, C_3S), while ferrochrome slag contains more magnesium silicates such as forsterite and monticellite. In general, both are non-metallic, glassy by-products with slower hydration than ordinary Portland cement (Siddique and Bennacer, 2012; Humad *et al*., 2019). In terms of chemical content, this by-product is composed of silicates, calcium aluminosilicates, and other phases, components are similar to Portland cement oxides (Puertas *et al*., 2000; Humad *et al*., 2019).

Replacing part of the clinker with steel or ferrochrome slag is currently applicable and brings several benefits, such as improved compressive strength. The degree of this enhancement depends on slag content, origin, and environmental exposure conditions (Lee *et al*., 2015), and is strongly influenced by the mechanical and physical properties of the slag. Due to its pozzolanic nature, slag gradually consumes $Ca(OH)_2$ and strengthens the cement matrix, improving resistance to sulfate and chloride attack (Nicula *et al*., 2023). Studies have also shown that slag-modified concretes maintain their durability and mechanical performance under extended environmental exposure (Siddique and Kaur, 2012).

Driven by the growing focus on sustainability, steel and ferrochrome slags are becoming increasingly important for environmentally friendly cement production (Siddique and Kaur, 2012; Li *et al*., 2016). Their use aims to reduce environmental impact, minimize landfill disposal, and enhance resource efficiency in the construction sector. However,

regional variability in slag composition makes standardized utilization challenging. Addressing these issues through advanced characterization, activation methods, and supportive regulations is essential for wider industrial implementation.

Research suggests that slag reactivity can be improved through mechanical or chemical activation. Mechanical activation through fine grinding increases surface area and structural disorder, enhancing hydration and strength development (Singla *et al*., 2020). Chemical activation through alkaline agents such as NaOH or Na_2SiO_3 promotes dissolution of amorphous phases and the formation of aluminosilicate gels, improving early-age strength (Humad *et al*., 2019). Slag can also be blended with other supplementary cementitious materials such as fly ash or limestone to improve long-term durability and resistance to aggressive environments (Ho and Huynh, 2024; Campagiorni *et al*., 2025).

Future studies must focus on creating cost-effective activation methods and assessing life cycle effects in order to fully utilize slag in sustainable cement production. This has both technical and environmental advantages due to continuous improvements in material characterization and processing methods (Tole *et al*., 2019). In this case, the study aims to characterize the properties of ferro-chrome and steel slags from Albania's metallurgical sector and evaluate their performance as partial replacements within the cementitious binder system to promote eco-efficient cement production.

2 Materials and methods

In this study, slag samples were evaluated alongside with ordinary Portland cement (OPC) to evaluate their physical and chemical characteristics, as well as their impact on compressive strength. The materials used were provided as-is and tested to evaluate their suitability for use in cementitious systems.

2.1 Materials collection

Multiple samples were collected for testing, with their origins detailed below:

- Two types of slags (black and white) were sourced from the steel manufacturing facility, located in Bradashesh, Elbasan, Albania.
- An additional slag sample originated from the ferrochrome production plant, also situated in Bradashesh, Elbasan, Albania.
- The reference cement (CEM I 42.5 R), used as the control binder, was obtained from the Fushe-Kruja Cement Factory in Fushe-Kruje, Albania.

a)

b)

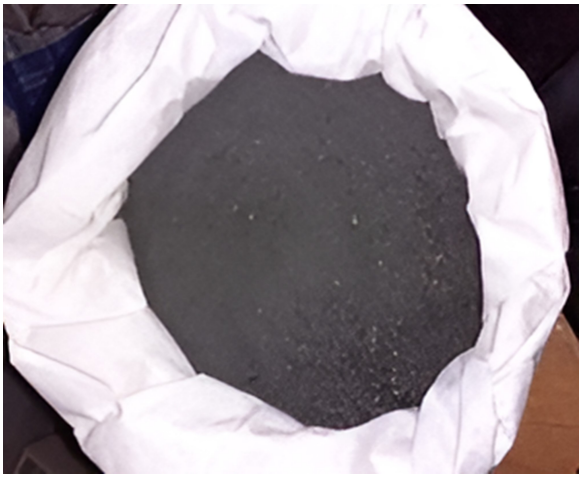

c)

Figure 1. a). Ferro-chrome (Fe-Cr) slag, b). white steel slag and c). black steel slag.

2.2 Sample Preparation and Mortar Formation

2.2.1 Sample preparation

The reproducibility and reliability of the test depend upon producing the samples properly. The intent is to have all of the slag samples compositionally homogeneous, and within the physical specifications necessary for the analysis. Samples were crushed to a particle size of less than 10 mm using a jaw crusher for sampling uniformity. Once crushed, they were ground using a ball mill at 1000 rpm, to obtain the desired particle size. The fine grind of the sample creates additional surface area which is critical in increasing the reactivity of the slag, and thereby providing the appropriate reaction rate for the chemical reactions to occur.

2.2.2 Mortar Mix Composition

The cementitious binder used in the mix consists of 520 g CEM I, 10 g gypsum, 170 g limestone and 300 g slag, totaling 1000 g. Those proportions were weighed and measured to ensure appropriate proportions for the intended application. For each mortar batch used to prepare three prism samples, the mix consisted of 450 ± 2 g of binder, 1350 ± 5 g of sand and 225 ± 1 g of water (CEN, EN 196-1:2016).

2.3 Chemical and Physical Characterization of Raw Materials

2.3.1 Chemical Composition (XRF Analysis)

The chemical composition of the samples, especially the key oxides which include CaO, SiO_2, Al_2O_3, and Fe_2O_3 (CEN, EN 196-2:2013), was determined using X-ray fluorescence (WD-XRF) spectrometer (PANalytical Axios mAX). Calibration curves were developed using at least six certified reference standards covering a wide range of oxide concentrations. The instrument was operated under standard cement-analysis conditions (nominal 60 kV and 125 mA) and controlled by SuperQ analytical software employing the least-squares regression method for calibration. For each measurement, 9 g of slag sample were mixed with 1 g of Boreox, homogenized in a porcelain mortar, and pressed into 32 mm diameter pellets under a 12-second automatic pressing cycle using a hydraulic press. The pressed pellets were cleaned with a soft brush before being placed in the XRF sample chamber. The SuperQ software automatically converted the measured X-ray intensities (kcps – kilocounts per second) into oxide concentrations based on the established calibration curves. Each sample was analyzed in triplicate, and the mean oxide composition (wt.%) was reported.

2.3.2 Mineralogical Composition (XRD Analysis)

The mineralogical phases of the samples were analyzed using a Bruker D8 Advance diffractometer equipped with a LynxEye SSD160 (1D) detector and Cu Kα radiation (λ = 1.5406 Å) operating at 40 kV and 40 mA. Diffraction data were collected in coupled $2\theta/\theta$ geometry over a range of 5°–60° (2θ) with a step size of 0.02° and 1 s per step. Finely ground powders were placed in standard holders to ensure a uniform surface. Phase identification was performed using Profex v6.0.3 (BGMN interface) with reference data from the Crystallography Open Database (COD).

2.3.3 Blaine Fineness Measurement

The specific surface area of the cement and slag samples was determined using a manual Blaine air permeability apparatus, following the procedure described in CEN, EN 196-6:2018. The method is based on measuring the time required for a fixed volume of air to pass through a compacted bed of powder under specified conditions. Approximately 2.5 ± 0.01 g of sample was weighed using an analytical balance (accuracy ±0.0001 g). The permeability cell had an internal diameter of 12.7 mm and a height of 15 mm, and was fitted with two filter papers at both ends. The sample was compacted with a smooth stainless-steel plunger (rod) of 12.65 mm diameter. The air flow time (t, in seconds) was measured between two calibration marks. Each test was repeated three times, and the average Blaine fineness (cm^2/g) was calculated. The Blaine fineness values were used to assess the reactivity potential of the slag samples, as higher fineness corresponds to increased hydration rate and strength development.

2.4 Fresh Properties of Cement–Slag Mortars

2.4.1 Water demand and setting time

The normal consistency and setting times of the cement and slag pastes were determined according to CEN EN 196-3:2016. A manual Vicat apparatus was used for water demand, and an automatic Vicatronic device for setting time measurement. For each test, 450–500 g of binder, sufficient to fill the Vicat mold (80 mm diameter, 40 mm height), was mixed with the required water to form a uniform paste. Tests were performed under controlled conditions of (20 ± 1) °C and (90 ± 5) % relative humidity. Normal consistency was defined as the water content that allowed the Vicat plunger (10 ± 0.05 mm diameter, 50 mm long) to penetrate to 6 ± 1 mm from the bottom of the mold. The initial setting time corresponded to a 1 mm needle penetration of 35 ± 1 mm, and the final setting time to the point where no surface mark remained. Each test

was run in triplicate, and average values were reported to evaluate the effect of slag replacement on hydration and setting behavior.

2.4.2 Workability determination procedure

The workability of the cement and slag mortars was evaluated using a manual mechanical flow table apparatus, following the procedure described in CEN EN 1015-3:1999. The device operated through a lifting mechanism with a drop height of 10 ± 0.2 mm. The conical mold used was 60 mm in height, with a top diameter of 70 mm and a bottom diameter of 100 mm, in accordance with the standard. Approximately 300 ± 5 g of mortar was placed into the greased mold in two layers, each compacted with 10 strokes of a 10 mm steel tamping rod. After leveling the surface with a trowel, the mold was lifted vertically, and the table was dropped 15 times at a rate of one drop per second. The spread diameter was measured along two perpendicular axes, and the average value was recorded as the flow (mm). Each test was performed in triplicate, and mean values were reported. Workability was used to evaluate the influence of slag on the rheological behavior and mix performance of the mortars.

2.5 Reactivity and Pozzolanic Behavior

2.5.1 Pozzolanic Activity Test

The pozzolanic activity of the slag samples was evaluated according to CEN EN 196-5:2011. The test was based on measuring the calcium hydroxide concentration in a saturated $Ca(OH)_2$ solution after contact with finely ground slag. Approximately 1.00 ± 0.01 g of slag was mixed with 75 mL of saturated $Ca(OH)_2$ and maintained under controlled lab conditions, with periodic agitation to ensure homogeneity. The suspensions then were filtered, and the $Ca(OH)_2$ concentration was determined by acid–base titration using 0.1 N HCl with phenolphthalein indicator. The reduction in $Ca(OH)_2$ concentration relative to the blank solution was used as an indicator of pozzolanic reactivity. This test provides data to determine the suitability of the slag as a partial cement replacement in low-carbon cement formulations.

2.6 Mechanical Performance

2.6.1 Mortar mixing and sample formation for testing

The components were combined in a mixing bowl and stirred for about 10 seconds to minimize any loss. Mixing started immediately once the water and cement made contact. Sand was added after 30 seconds and stirred for an additional 30 seconds. After turning the mixer up to its highest setting, mixing went on for an additional 30 seconds. Then using a rubber spatula, the mixing was stopped for 90 sec to scrape off any mortar left on the walls. All the material was collected in the center before mixing resumed at full speed for 60 sec. Specimens were cast as prisms measuring 40 mm x 40 mm x 160 mm, prepared immediately after mixing. The mold was fixed to the impact table, and compacted with 60 strokes, and the molds were stored in a humidity cabinet. Finally, the prisms were cured in water baths maintained at 20.0 ± 1.0 °C. For tests after 24 hours, samples were removed from the molds no more than 20 minutes before compressive strength measurement (CEN, EN 196-1:2016).

2.6.2 Compressive strength analysis

Initially, a metal cube is placed, and the press is pre-loaded to 100 kN. The prism is then positioned in the device designed for bending fracture. Following the fracture, the resulting half-prism is centered on the side faces of the machine plates, with an alignment tolerance of ± 0.5 mm. The half-prism is oriented longitudinally so that its last face protrudes approximately 10 mm above the plate.

Figure 2. a). Leveling tools, b). humidity cabinet, c). prisms (40 mm x 40 mm x 160 mm).

Table 1. Oxide composition of ferro-chrome, black and white slag.

	MgO %	Al_2O_3 %	SiO_2 %	CaO %	TiO_2 %	MnO %	$Fe2O_3$ %
Fe-Cr Slag	10.33	6.567	16.02	1.2	0.1	10.34	0.29
Black Slag	9.922	12.61	20.91	38.91	0.72	11.24	14.39
White Slag	9.63	11.34	21.77	45.66	0.51	1.861	11.92

Table 2. Oxide composition of CEM I 42.5R (control sample).

	Al_2O_3 %	CaO %	SiO_2 %	MgO %	Fe_2O_3 %	TiO_2 %	Na_2O %	P_2O_5 %	SO_3 %	L.O.I %
CEM I 42.5R	4.29	59.61	16.39	3.01	2.66	0.65	0.23	0.21	2.8	1.87

The specimen is then subjected to loading in the press at a rate of 2400 ± 200 N/s by adjusting the press function. Automatic pressing is applied to the half-prism under load, and the result is recorded in MPa, where 1 MPa is defined as the force exerted divided by the area in mm^2 (CEN, EN 196-1:2016).

3 Results

3.1 The oxide composition of the samples (XRF results)

A comparative summary of the major oxide contents for the slag samples and the ordinary Portland cement (CEM I 42.5R) is presented in Tables 1 and 2.

According to the oxide composition results, the white steel slag is the richest in the three major oxides (Ca, Al, and Si). This sample, with a high CaO content (45.66%) and with moderate quantities of SiO_2 and Al_2O_3, could be the most promising slag from a cementing perspective. The higher CaO promotes the formation of calcium silicate hydrates (C-S-H), which provide for a stronger cement matrix in terms of durability and compressive strength, consistent with observations by Lothenbach *et al*. (2011) and Puertas *et al*. (2000).

Regarding iron, reported as Fe_2O_3, it is substantial in both steel slags and only slightly lower in the white slag (≈11.9%) than in the black slag (≈14.4%). Elevated total iron has been shown to influence hydration kinetics and slag reactivity, as observed by Lothenbach *et al*. (2011) and Humad *et al*. (2019), who reported that Fe-rich slags exhibit slower reaction rates and reduced strength development. On the other hand, the black slag presents moderate CaO, and higher Fe_2O_3 content that may affect the setting times and early strength development (Lee *et al*., 2015; Humad *et al*., 2019). Thus, it would give some cementitious reactivity but may need further optimization or activation. The ferrochrome (Fe-Cr) slag, characterized by low CaO but elevated MgO and MnO, is less efficient in forming strength-giving hydrates under normal conditions. Its chemistry corresponds to the predominance of dense, crystalline phases and spinel-type oxides, which are known to exhibit low hydraulic reactivity and may induce expansion if not stabilized, as also reported by Tripathi *et al*. (2025). Similar observations on MgO-rich industrial residues with limited cementitious behavior were discussed by Das *et al*. (2021), highlighting the need for activation treatments to improve their reactivity. The CEM I 42.5R exhibits a significantly higher CaO content than the slag samples, which is consistent with rapid early hydration driven by clinker phases and contributes to the higher early strength of the control (Kurdowski, 2014); Hewlett & Liska (2019).

3.2 Mineralogical Composition (XRD Analysis)

The XRD patterns of CEM I 42.5R and the slag samples are presented in figure 3.

CEM I 42.5R exhibits typical alite (C_3S) and belite (C_2S) peaks, with minor C_3A, C_4AF, gypsum, and portlandite. These phases explain its rapid hydration and strength development through C-S-H and portlandite formation, as discussed by Scrivener *et al*. (2019).

The white steel slag shows portlandite, C_2S, merwinite, and gehlenite, with minor CaO and C_2F. Its Ca-rich mineralogy and limited Fe-bearing phases confirm a high content of reactive silicate and aluminate structures, indicates potential hydraulic reactivity, and strength efficiency compared with the other slags, consistent with observations by Kriskova *et al*. (2013) and Vlček *et al*. (2016).

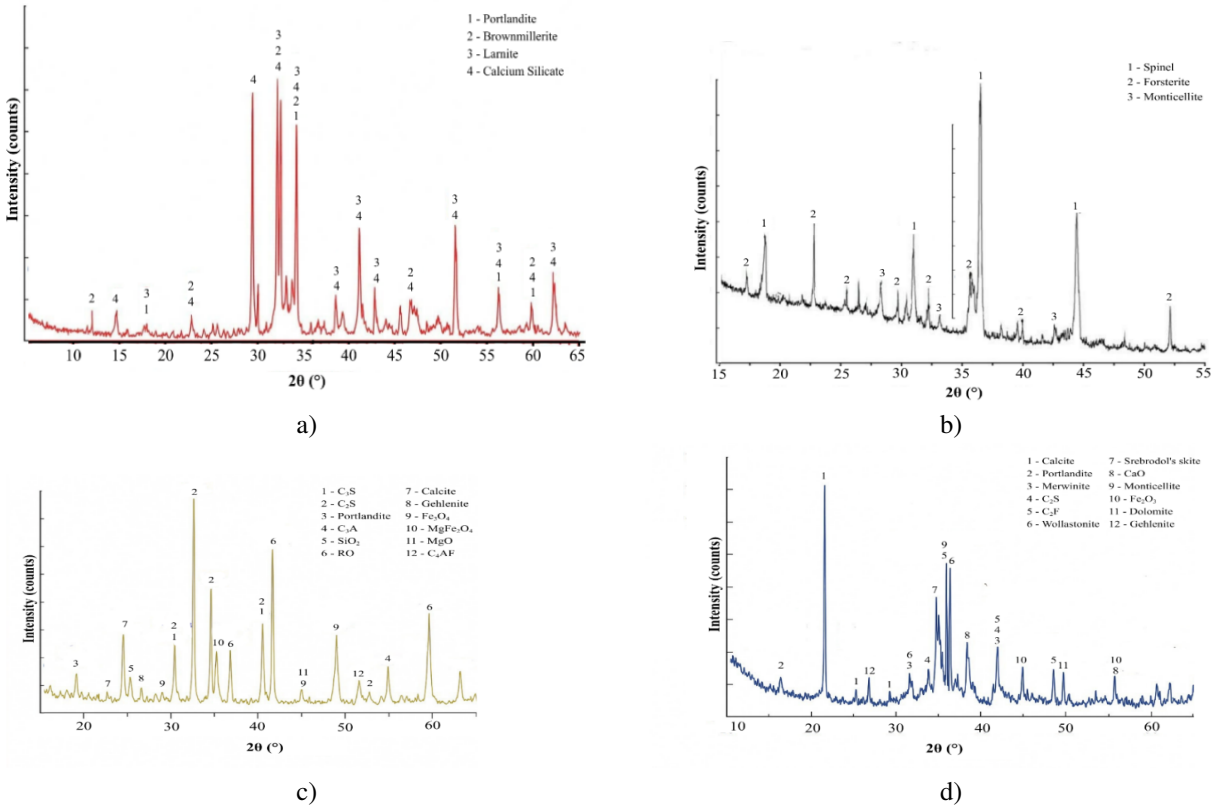

Figure 3. XRD patterns of a). CEM I 42.5R, b). Fe-Cr slag, c). white steel slag and d). black steel slag.

Table 3. Specific gravity, Blaine fineness, and bulk density results for all samples.

Parameter	CEM I 42.5R	Black Slag	White Slag	Ferro-Cr Slag
Specific Gravity [g/cm^3]	3.15	3.10	3.05	3.25
Blaine Fineness [cm^2/g]	3728	3700	3900	3200
Bulk Density [kg/m^3]	1480	1500	1450	1550

The black steel slag is characterized by C_2S, Fe, Mg and Mn RO ((Fe,Mn,Mg)O), ferrite phases (C_4AF, C_3A), and spinels (Fe_3O_4, $MgFe_2O_4$). The presence of such Fe, Mg and Mn bearing RO and ferrite structures, reported also by Zhang *et al*. (2024), Zhuang and Wang (2021), and Eba *et al*. (2021), is known to hinder hydration by forming dense, inert crystalline matrices that limit water penetration and delay silicate activation. This microstructure explains the slower hydration and reduced early strength gain observed in black slag.

The ferrochrome slag primarily contains Mg-Fe-Cr spinels ($(Mg,Fe)(Cr,Al)_2O_4$), forsterite ($(Mg,Fe)_2SiO_4$), and monticellite ($CaMgSiO_4$). These olivine and spinel type minerals are thermodynamically stable, refractory, and largely inert toward hydration, which explains the low pozzolanic activity of Fe-Cr slags. Similar mineral compositions have been described by Karhu *et al*. (2020) and Das *et al*. (2023), confirming that such crystalline phases originate under highly reducing and high temperature ferroalloy conditions, resulting in poor reactivity and filler type behavior when incorporated into cementitious systems.

3.3 Assessment of specific gravity, blaine fineness and bulk density

The table below presents the specific gravity, Blaine fineness, and bulk density values for CEM I 42.5R, black and white steel slag, and ferro-chrome slag. Each measurement was performed in triplicate, and the average value is reported.

The Fe–Cr slag shows the highest specific gravity, consistent with the presence of dense spinel/olivine phases typical of ferroalloy slags, as also identified in the XRD analysis (Section 3.2) and reported by Holappa and Xiao (2004) and Karhu *et al*. (2020). Its high MgO content and mineralogical composition correspond to reduced hydraulic reactivity, which is characteristic of these thermodynamically stable phases (Das *et al*., 2023).

Table 4. Water demand and setting time results for CEM I 42.5R and slag-based binders.

Parameter	CEM I 42.5R	Black Slag	White Slag	Ferro-Cr Slag
Water Demand (ml)	126	144	171	189
Initial Setting Time (min)	110	140	180	250
Final Setting Time (min)	230	250	300	350

The distinct mineralogical compositions of the steel slags and CEM I are indicated by their relatively lower specific gravities. Because of its highest Blaine fineness, the white steel slag appears to have been finely ground, increasing its surface area and promoting cement hydration and reactivity. Additionally, its mineral composition may facilitate grinding, because it contains more soft and brittle calcium-rich compounds (Section 3.2) compared with the Fe-rich black slag, where harder Fe-bearing crystalline phases (ferrites and spinels) can hinder grinding efficiency. This observation aligns with Zhao *et al*. (2017), who reported that the presence of Fe-rich phases reduces the grindability of steel slags. Similarly, Ryu *et al*. (2024) noted that Fe-rich slags containing ferrites and spinels tend to exhibit hardness and reduced grinding efficiency compared with other slags such as LFS and BFS.

The shapes, packing and intrinsic densities of the particles cause the variations in bulk density which, range from 1450 kg/m^3 for white slag to 1550 kg/m^3 for ferro-chrome slag. These physical attributes show how processing and chemical composition interact to influence the performance of these materials in cement-based systems.

3.4 Water demand, initial and final setting time results

Below, water demand, initial, and final setting time values for mortar mixtures prepared with CEM I 42.5R and slag-based binders, is presented. These properties are essential indicators of workability and hydration behavior, influencing mixing, and placing. Tests were repeated three times and the mean results are reported.

Water demand and setting times are influenced by the material's physical properties such as bulk density, specific gravity, and Blaine fineness, as well as their chemical composition and mineralogy.

Compared to ordinary Portland cement, steel slags generally exhibit slower hydration kinetics because their crystalline phases are dominated by belite (C_2S) rather than alite (C_3S). As shown in Section 3.2, CEM I 42.5R contains more C_3S, which hydrates rapidly and sets early, whereas slags contain ferritic, spinel structures that hydrate more slowly. This compositional difference, rather than fineness alone, explains the delayed setting behavior (Scrivener *et al*., 2019; Lothenbach *et al*., 2011).

The white steel slag, with its higher Blaine fineness, shows increased water demand because of its greater surface area and more porous particle morphology. Yet, its setting times remain longer due to the slower hydration of its crystalline and gehlenite phases compared to C_3S. Lothenbach *et al*. (2011) noted that belite reacts slowly, producing C-S-H at a slower rate and thus delaying strength development. Likewise, Borges Marinho *et al*. (2017) and Chang *et al*. (2019) measured setting times of mortars incorporating LFS and reported delayed setting relative to OPC controls, consistent with the lower early reactivity of gehlenite/merwinite-bearing LFS.

The Fe-Cr slag, despite its high specific gravity, shows the longest setting times owing to its low CaO content and the predominance of inert spinel and forsterite phases (Section 3.2). These phases do not contribute to early hydration, leading to delayed setting. The high MnO content further influences hydration by promoting formation of mixed RO and spinel phases, as indicated by the XRD results.

These low-solubility, weakly hydraulic phases form diffusion-limiting surface layers that reduce available sites for C-S-H formation, thereby extending both initial and final setting times. Zhuang *et al*. (2021) demonstrated that Fe-rich RO, ferrite and spinel phases form dense interfacial layers that impede ion transport and inhibit early-age hydration of cement, and Yan *et al*. (2022) further showed that high-FeO, MnO RO encapsulates silicate phases and suppresses hydration, while Holappa and Xiao (2004) described such spinel-type minerals in ferrochrome slags as thermodynamically stable and refractory. Consistent with this behavior, recent reviews have confirmed that Fe-Mn-Mg rich slags generally require mechanical or chemical activation to enhance their hydraulic performance (Das *et al*., 2023; Karhu *et al*., 2020). Collectively, these results confirm that both physical and mineralogical factors, rather than fineness alone, control the hydration kinetics of steel slags.

3.5 Evaluation of cement and slag-based mixtures

The following graph presents the workability results of mortar mixtures prepared with CEM I 42.5R and slag-based binders, measured in terms of flow (cm) and relative workability (%). Workability affects the ease of handling, mixing, placing, and finishing concrete or cementitious materials.

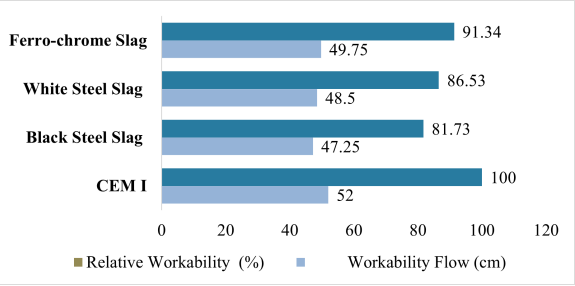

Figure 4. Graphical presentation of workability flow and relative workability results of CEM I 42.5R and slag-based binders.

Measurements were obtained in triplicate, with the average value used for comparison.

The results show that CEM I exhibits the highest flow and relative workability, most likely as a result of its optimized fineness and chemical composition (high CaO content) that promote early hydration and fluidity (Scrivener *et al*., 2019; Lothenbach *et al*., 2011).

The Fe–Cr slag formulation showed comparatively good workability among the slag mixes despite its highest water demand. This behavior is consistent with its lower Blaine fineness and relatively smooth particle morphology, which decrease inter-particle friction and facilitate flow. Das *et al*. (2023) discussed that ferrochrome slags containing spinel and olivine-type minerals often display rounded or sub-angular particle textures, which may contribute to maintaining acceptable flowability even though their hydraulic reactivity is limited.

The white and black slag formulations have lower workability, correlated with their higher Blaine fineness and angular particle geometry, which increase surface area and water adsorption (Najm *et al*., 2021). The white slag's higher CaO and SiO_2 contents raise water demand and promote surface hydration films, causing reduced flowability, whereas the Fe, Mg and Mn rich black slag develops dense ferritic and spinel phases that reduce surface hydration and particle mobility (Zhuang *et al*., 2021; Yan *et al*., 2022). Zhuang *et al*. (2021) demonstrated that Fe-rich RO, ferrite and spinel phases form dense interfacial layers that impede ion transport and inhibit early-age hydration of cement, while Yan *et al*. (2022) showed that high FeO, MnO RO encapsulates silicate phases and suppresses hydration mechanisms consistent with the reduced mobility and workability observed here. Overall, these results confirm that workability in slag-cement systems is influenced by fineness, chemical composition and particle morphology. These observations are consistent with Ryu *et al*. (2024), who noted that microstructural characteristics and Fe/Mn/Mg-rich phases significantly influence both rheology and hydration performance of steel and ferroalloy slags.

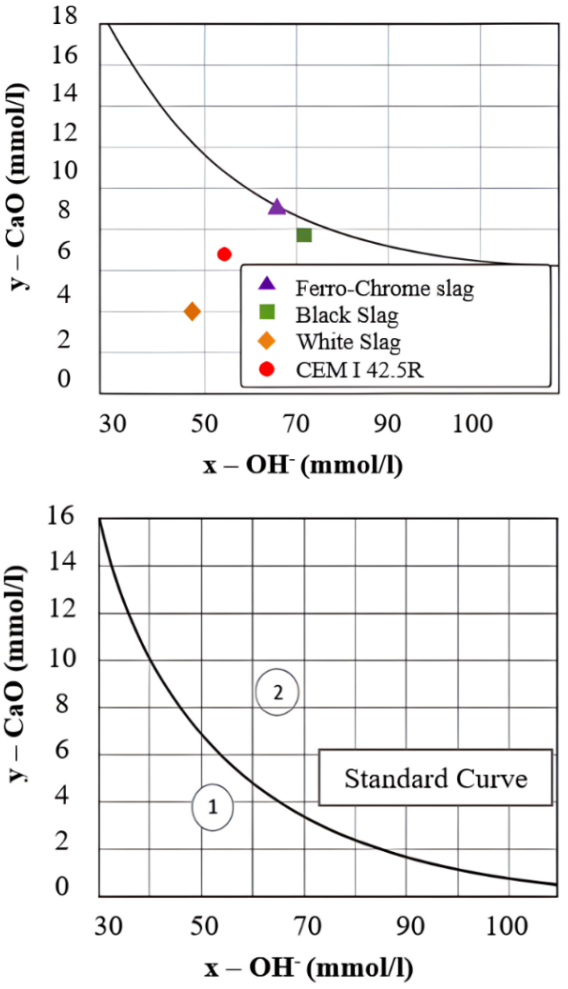

Figure 5. a). Pozzolanity activity representation for all samples, and b). standard curve.

3.6 *Pozzolanic activity test results*

The graph demonstrates the pozzolanic properties of the samples according to their CaO and OH^- levels in relation to the lime solubility curve. It indicates the pozzolanic chemical behavior of each sample, which generally correlates with their compressive strength and pozzolanic activity index (PAI) values. For pozzolanity to be confirmed, the data points must fall below the standard solubility curve, which serves as a reference (Taylor, 1997; EN 196-5).

Samples positioned lower and to the left, such as CEM I 42.5R and white slag, indicate greater calcium hydroxide (CH) consumption and thus higher pozzolanic or latent-hydraulic reactivity. This trend aligns with their compressive strength values shown in the following section. The higher reactivity of the white slag, despite its moderate CaO content, is attributed to its reactive silicate and aluminate phases (C_2S, gehlenite, and merwinite), which effectively consume CH during hydration, thereby utilizing the $Ca(OH)_2$ released from CEM I to form additional C-S-H (Jacob, 2024; Vlček *et al*., 2016).

Table 5. Compressive strength (MPa) of all mortars after 2, 7, 14, and 28 days, with mean, standard deviation (SD), and coefficient of variation (CV). (M.1-M.3 = replicate tests).

Mix	Age (days)	M.1 (MPa)	M.2 (MPa)	M.3 (MPa)	Mean (MPa)	SD (MPa)	CV (%)
CEM I 42.5 R (Control)	2	26.7	25.4	25.9	26	1.04	4
	7	39.8	37.9	37.8	38.5	1.46	3.8
	14	45.4	43.7	43.5	44.2	1.5	3.4
	28	49.5	47.1	47.7	48.1	1.63	3.4
70 % CEM I + 30 % Fe-Cr Slag	2	19	17.7	18.1	18.3	0.73	4
	7	27.8	26.1	26.4	26.8	1.02	3.8
	14	31.4	29.9	30.6	30.6	1.04	3.4
	28	34.2	32.4	32.5	33	1.12	3.4
70 % CEM I + 30 % Black Slag	2	14.9	13.6	13.8	14.1	0.56	4
	7	22.9	21.2	21.6	21.9	0.83	3.8
	14	27.3	25.5	26	26.3	0.89	3.4
	28	31.2	29.3	29.5	30	1.02	3.4
70 % CEM I + 30 % White Slag	2	18.8	17.4	17.8	18	0.72	4
	7	30.2	28.4	28.7	29.1	1.11	3.8
	14	36.7	35	35.8	35.8	1.22	3.4
	28	43.2	41.1	41.7	42	1.43	3.4

In contrast, Fe-Cr and black slags, located close to the solubility line, show limited reactivity and lower compressive strength, confirming the consistency between their chemical and mechanical behavior. The main reason for the low pozzolanic reactivity of the black slag is likely its high Fe_2O_3 content, despite having a moderate CaO%. Iron oxides can inhibit dissolution reactions that are essential for C-S-H formation, thereby reducing hydration and strength gain (Zhuang *et al*., 2021; Yan *et al*., 2022). The Fe-Cr slag exhibits even lower reactivity, mainly due to its low CaO content and high proportion of spinel and forsterite phases, which are thermodynamically stable and inert under standard hydration conditions (Holappa & Xiao, 2004; Das *et al*., 2023).

3.7 Compressive strength results

Compressive strength analysis is one of the key indicators which helps identify the structural quality and durability of cementitious materials, influencing directly the material's capability to resist mechanical loads and external stresses over time. This information is crucial for assessing the performance of the material in construction applications, as well as the compliance with standards for specific engineering applications.

3.7.1 Compressive strength results for mortars with slag-based binders and CEM I 42.5R

Table 5 summarizes the corresponding compressive strength data (MPa), including mean values, standard deviations (SD), and coefficients of variation (CV). Each reported value represents the average of three replicate measurements. The obtained standard deviations (0.6–1.6 MPa, corresponding to CV ≈ 3–4%) lie within the repeatability limits defined by ASTM C109. Figure 6 compares the compressive strength evolution of mortar mixtures prepared with slag-based binders and CEM I 42.5R after 2, 7, 14, and 28 days of curing, providing a clear visual representation of strength development over time.

The compressive strength analysis showed that the control sample (CEM I 42.5R) achieved the highest strength at all tested intervals (2, 7, 14, and 28 days), primarily due to its optimized chemical composition, fine particle size, and rapid hydration kinetics that promote early C-S-H formation, as also reported for C_3S rich Portland cements by Scrivener *et al*. (2019) and Lothenbach *et al*. (2011).

The mixture containing 30% Fe-Cr slag exhibited moderate early strength at 2 days, which can be attributed not to chemical reactivity but to a physical filler and densification effect that improves packing and reduces porosity at early ages. Early age strength gains via filler-induced packing are well established (Berodier & Scrivener, 2014; Bentz, 2017). This interpretation is consistent with the XRD results, which confirmed the dominance of inert spinel and forsterite phases, which are known to be thermodynamically stable and non-reactive under normal hydration conditions (Das *et al*., 2023; Karhu *et al*., 2020). These phases act primarily as microfillers rather than reactive components, explaining the transient early strength despite limited long-term hydration reactivity.

The black steel slag mixture showed the lowest strength performance, consistent with its higher Fe_2O_3 and MnO contents that inhibit silicate hydration and pozzolanic reactions (Yan *et al*., 2022; Zhuang *et al*., 2021). Despite a moderate fineness, these Fe-bearing phases form diffusion-limiting layers that impede ion transport and delay C-S-H formation, explaining the slower strength gain.

Conversely, the mixture containing 30% white slag performed significantly better, due to its higher Blaine

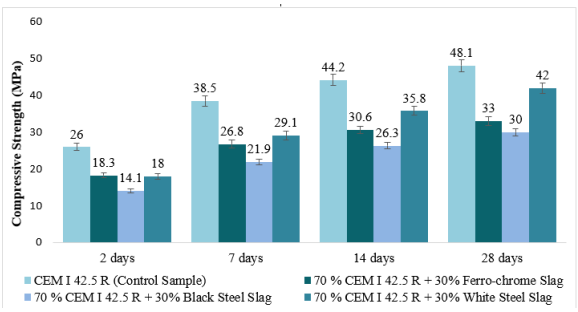

Figure 6. Compressive strength comparison for CEM I 42.5 R and slag-based formulations after 2, 7, 14 & 28 days. Values are means of n = 3; error bars = ±SD; CV ≈ 3–4%).

fineness and reactive mineral phases (C_2S, gehlenite, merwinite), which consume $Ca(OH)_2$ released from CEM I hydration and generate additional C-S-H. This mechanism enhances both pozzolanic efficiency and long-term strength (Jacob, 2024; Vlček *et al*., 2016).

These variations show how chemical composition, fineness, and physical properties interact to influence hydration kinetics and strength development. For 30% replacement rate slag-based mixtures generally exhibit slower early strength gain than the control sample.

3.7.2 Strength efficiency per unit CaO content

In addition to determining compressive strength, the effectiveness of calcium oxide (CaO) utilization was evaluated. This was done by normalizing the compressive strength values with the corresponding CaO content, providing an indication of how efficiently available calcium contributes to hydrate formation and overall strength. Calcium oxide, released during the hydration of alite (C_3S) and belite (C_2S), forms the principal binding phases, calcium silicate hydrate (C-S-H) and portlandite (CH), which influence mechanical performance (Taylor, 1997; Scrivener *et al*., 2019; Hewlett & Liska, 2019):

$$2C_3S + 6H \rightarrow C_3S_2H_3 + 3CH$$

$$2C_2S + 4H \rightarrow C_3S_2H_3 + CH$$

In blended systems, secondary C-S-H forms through the pozzolanic reaction between CH and reactive silica or aluminosilicate phases present in the slag, where *S* represents the reactive component of the slag (EN 196-5; Lothenbach *et al*., 2011):

$$CH+S+H \rightarrow C\text{-}S\text{-}H$$

To compare binders with different CaO contents, a non-standard interpretive parameter, strength per unit CaO (MPa per % CaO), was introduced. This metric reflects how effectively each binder converts available or released CaO into strength-forming hydrates.

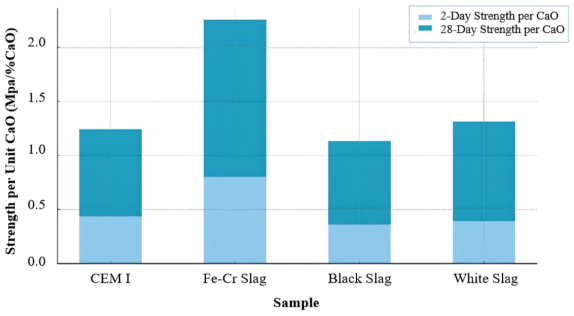

Figure 7. Cumulative compressive strength per unit CaO content at 2 and 28 days for all binder systems.

As shown in Figure 7, although CEM I achieved the highest absolute strength, its lower strength-per-CaO ratio suggests that its performance is primarily driven by its higher CaO content, rather than superior chemical efficiency.

The white slag blend shows the greatest CaO efficiency despite having less total CaO. This is attributed to its reactive Ca-bearing phases (C_2S, gehlenite, merwinite), which, in the presence of Portland cement, react with the $Ca(OH)_2$ released during hydration to form additional C-S-H and C-A-S-H gels, enhancing reactivity (Jacob, 2024; Vlček *et al*., 2016; Lothenbach *et al*., 2011). Remarkably even though the Fe-Cr slag blend exhibited the lowest absolute strength, it showed relatively a high CaO efficiency particularly in the early stages, likely due to filler-induced densification and localized surface hydration of minor reactive phases (Berodier & Scrivener, 2014; Bentz, 2017). Although its overall strength is likely limited by factors such as coarse fineness and composition, the results indicate that its limited CaO content is used effectively.

Whereas the black slag, rich in spinel and RO phases, shows limited CaO utilization because of low hydration and restricted CH consumption (Yan *et al*., 2022; Zhuang *et al*., 2021). Reactivity, fineness, and phase composition of the blends, affect compressive strength in addition to the CaO content as highlighted in this analysis.

3.7.3 Power law modelling of long-term compressive strength development

In this section, a statistical prediction of compressive strength development up to 90 days for all samples is presented**,** using the empirical power law $y = a \cdot x^b$, where a represents the early-age strength coefficient and b the rate of strength gain over time. The curves were fitted to data obtained at 2, 7, 14, and 28 days, achieving R^2 values between 0.95 and 0.98, indicating a strong fit within the measured range. Variability was accounted for by applying uncertainty bands of ±10%. Predictions beyond 28 days are extrapolations and should be viewed as theoretical estimates, as strength gain typically slows

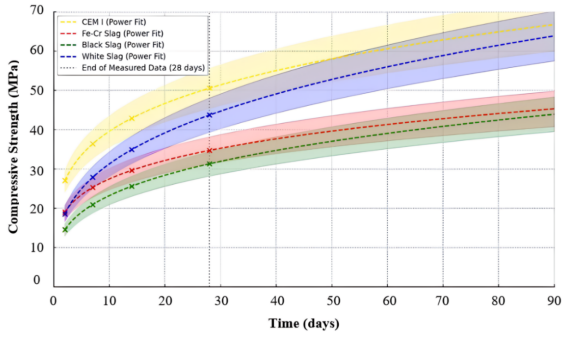

Figure 8. Predicted compressive strength evolution of all binder systems (2–90 days) based on power law model.

after 28 days (Thomas, 2013; Scrivener et al., 2019). The model is therefore intended only to illustrate comparative strength evolution trends.

The model predicts that the white slag blend would achieve the most consistent and sustained strength development, as indicated by its b-value and high R^2 model fit. CEM I exhibits the highest early strength due to its high a-value, but its strength growth is slower over time. Fe-Cr and black slag blends start lower and develop strength at different rates. Although the black slag blend's b-value suggests a relatively faster predicted growth rate than CEM I, its low early strength means it shows the slowest overall performance. In this context, the 'a' coefficient represents early strength potential, 'b' the progression of strength gain, and R^2 shows how closely the regression fits the experimental data. This demonstrates how both early reactivity and long-term gain vary across the binders.

3.7.4 Performance and reactivity of slag formulations in cement replacement

The percentage of compressive strength retained by the slag formulations, compared to the control sample (CEM I 42.5R), at 2, 7, 14, and 28 days is presented in the following graph. This offers a comparison of the compressive strength development over time and provides insight for the materials usage in certain applications.

At two days, all slag formulations exhibit decreased strength when compared to the control sample. The Fe-Cr slag blend showed the highest early-age relative strength followed by the white and black slag mixes. All of the blends show improvement by the 28-day mark, but white slag mixture demonstrates the most significant improvement, achieving 87.32% of the control sample's strength. From the results obtained, it is considered that despite initial strength development being slower than the control, slag-based formulations, especially those with white slag, demonstrate the potential to achieve 60% to 88% of the control's strength at 28 days.

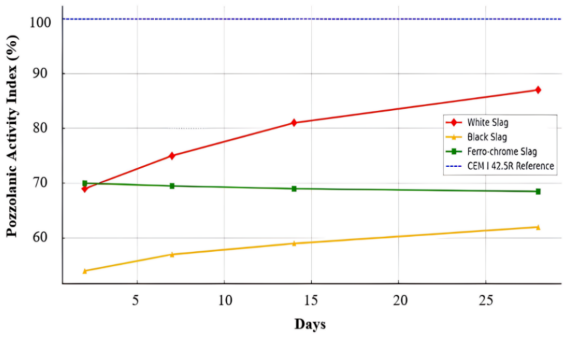

Figure 9. Evolution of pozzolanic activity index (%) over time for all slag blends.

Because of its balanced composition, favorable Blaine fineness, and high CaO content, the white slag blend shows the strongest pozzolanic behavior as also indicated by the pozzolanic activity index (PAI) curves. The higher FeO and MnO contents in the black slag likely inhibit reactivity, while the Fe-Cr slag, dominated by spinel and forsterite, acts mainly as an inert filler rather than a reactive component (Das *et al.*, 2023; Holappa & Xiao, 2004; Zhuang *et al.*, 2021).

In addition to performance comparison, a correlation heatmap (Fig. 10) was created to show how the important chemical and physical variables were correlated with the compressive strength of slag-containing cementitious systems. This provides an overview as to which properties are predominantly related to early and long-term compressive strength.

CaO's role in hydration and strength gain is confirmed by the positive correlation found between CaO content and both early (r = 0.82) and long-term (r = 0.87) compressive strength. Strength and relative workability also exhibit a positive correlation confirming the idea that well-optimized mixes promote improved reactivity and packing.

In contrast there is a significant negative correlation between water demand and strength performance (r ≈ –0.84 to –0.86) suggesting that higher water requirements could result in decreased strength performance.

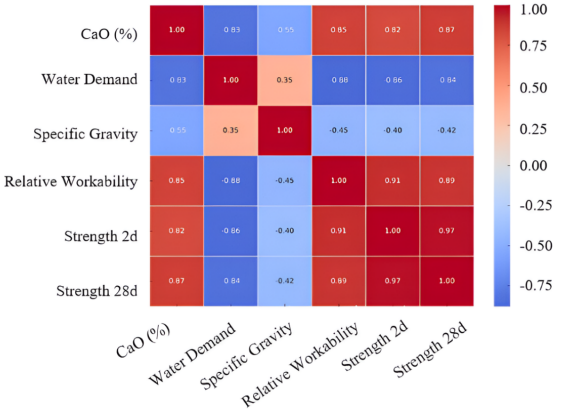

Figure 10. Correlation heatmap of key parameters influencing compressive strength.

Denser materials may not always translate into higher strength as evidenced by the modest inverse relationship between specific gravity and strength. This matrix gives a clear summary of the interconnected elements that affect mechanical behavior in blended binders and overall confirms trends that were already mentioned in the earlier sections.

4 Discussions

The mechanical performance of the slag-cement mortars is influenced by the phase composition (XRD), oxide chemistry (XRF), and fineness. Across all mixes, CEM I led at every age, consistent with the hydration behavior of C_3S and C_2S phases that promote rapid C-S-H and CH formation, as noted by Taylor (1997) and Scrivener *et al*. (2019).

Among the slags, white steel slag showed the most favorable performance due to (i) reactive Ca-bearing phases such as C_2S, gehlenite, and merwinite, (ii) the highest Blaine fineness, and (iii) balanced oxide composition. These factors enhanced $Ca(OH)_2$ consumption and secondary C-(A)-S-H formation, resulting in 87.3% of the control's 28-day strength and the highest strength per unit CaO (Jacob, 2024; Vlček *et al*., 2016; Lothenbach et al., 2011).

Black steel slag underperformed despite moderate CaO and fineness. Its Fe-Mn rich RO and spinel, ferrite phases create dense interfacial layers that slow dissolution of silicate phases and prevent ion transport, suppressing early C-S-H formation, a mechanism reported by Zhuang *et al*. (2021) and Yan *et al*. (2022) and consistent with our longer setting times, lower workability, and lower strengths.

Fe-Cr slag showed intermediate behavior: dominant Mg-Fe-Mn spinels, forsterite, monticellite are thermodynamically stable and inert, so early strength arises mainly from filler-induced packing and nucleation, rather than reactivity (Berodier & Scrivener, 2014; Bentz, 2017; Holappa & Xiao, 2004; Das *et al*., 2023; Karhu *et al*., 2020). This explains the moderate 2-day strength and low long-term gain, and the good flow despite high water demand.

Overall, CEM I maintained the highest early and total strength, but white slag showed potential as a 30% cement replacement. In contrast, black and Fe-Cr slags would require further activation (e.g., alkali treatment) or may serve better as fillers or aggregates where reactivity is less critical (Zhuang *et al*., 2021; Das *et al*., 2023; Karhu *et al*., 2020).

From a practical perspective, white slag shows potential for partial cement replacement at ≤30% level, requiring minimal processing changes, making large-scale use technically feasible and likely economically attractive, especially where steel slags are locally available.

In contrast, black and Fe-Cr slags show limited reactivity and would require additional activation (e.g., alkali treatment) to achieve comparable performance. These extra steps raise processing costs, reducing economic viability, though their use as fillers or aggregates in non-structural applications remains a sustainable option that supports circular economy goals (Zhuang *et al*., 2021; Das *et al*., 2023; Karhu *et al*., 2020).

As for the study limitations, to keep the focus on comparative performance, testing was conducted up to 28 days and at a single replacement level (30%), while aspects such as shrinkage, and leaching behavior remain to be explored. Further investigations could extend these findings by examining long-term durability, alternative activation routes, and variability between slag sources under industrial conditions, as highlighted in durability-focused studies on cementitious systems incorporating industrial by-products (Ramírez-Arreola *et al*., 2020).

Conclusions

1) Among the examined slags, white steel slag showed the most favorable combination of mineral reactivity and fineness, reaching 87.3% of the control's 28-day strength. Its high CaO efficiency, confirmed by XRD and pozzolanity tests, reflects effective participation of reactive Ca-silicate and aluminate phases in hydrate formation.

2) Black steel slag exhibited the lowest strengths, attributable to Fe, Mn-rich RO, ferrite, and spinel phases that inhibit hydration kinetics, consistent with the observed workability, setting trends and literature mechanisms.

3) Fe-Cr slag acted primarily as an inert microfiller, showing moderate early strength from packing effects but limited reactivity at later ages, in agreement with its spinel, forsterite and monticellite dominated XRD profile.

4) At a 30% replacement level, all slag blends showed lower absolute strength than CEM I. Across 2-28 days, black slag retained approximately 54-62% of CEM I strength, Fe-Cr slag retained 68–70%, and white slag retained 69-87%, with white slag showing the highest potential for low-carbon binders.

5) Slag incorporation increased water demand and delayed setting times relative to CEM I, consistent with their higher fineness and slower-reacting mineral phases.

6) White slag can be considered suitable for ≤30% cement replacement, subject to long-term durability and field validation. Black and Fe-Cr slags may be better used at lower replacement ratios, after mechanical or chemical activation, or as fillers/aggregates in non-structural applications.

7) Future work should include durability (sulfate, chloride, carbonation), stability, leaching, heavy-metal mobility, optimization of replacement levels, and validation beyond 28 days (e.g., 56/90 d) to confirm long-term behavior.

8) Overall, incorporating slags into cement offers a practical approach to reduce CO_2 emissions and recycle industrial by-products, supporting the development of greener, more sustainable cement formulations.

Acknowledgements

The authors are grateful to the specialists of Fushë-Kruja Cement Factory for their cooperation and assistance during all the experiments.

References

ASTM International. (2002). Standard test method for compressive strength of hydraulic cement mortars (ASTM C109/C109M-02). West Conshohocken, PA: ASTM International. https://doi.org/10.1520/C0109_C0109M-02

Bentz, D. P., Ferraris, C. F., Jones, S. Z., Lootens, D. and Zunino, F. (2017). Limestone and silica powder replacements for cement: Early-age performance. *Cement and Concrete Composites*, 78, 43–56. https://doi.org/10.1016/j.cemconcomp.2017.01.001

Berodier, E. and Scrivener, K. (2014). Understanding the filler effect on the nucleation and growth of C–S–H. *Journal of the American Ceramic Society*, 97(12), 3764–3773. https://doi.org/10.1111/jace.13177

Borges Marinho, A. L., Mol Santos, C. M., Franco de Carvalho, J. M., Castro Mendes, J., Brigolini, G. J. and Fiorotti Peixoto, R. A. (2017). Ladle furnace slag as binder for cement-based composites. *Journal of Materials in Civil Engineering*, 29(11), 04017206. https://doi.org/10.1061/(ASCE)MT.1943-5533.0002061

Campagiorni, L., Tonelli, M. and Ridi, F. (2025). Synergistic effect of limestone and supplementary cementitious materials in ternary blended cements. *Current Opinion in Colloid & Interface Science*, 75, 101885. https://doi.org/10.1016/j.cocis.2024.101885

Chang, S. Y., Chen, C. S., Tu, C. H. and Tseng, Y. W. (2019). Ladle furnace slag as a sustainable binder for masonry mortars. *Key Engineering Materials*, 801, 385–390. https://doi.org/10.4028/www.scientific.net/KEM.801.385

Das, S. K., Mishra, S., Das, D., Mustakim, S. M., Kaze, C. R. and Parhi, P. K. (2021). Characterization and utilization of coal ash for synthesis of building materials. In *Clean Coal Technologies*, 487–509. Springer Nature. https://doi.org/10.1007/978-3-030-68502-7_19

Das, S. K., Mustakim, S. M., Adesina, A. and Mishra, S. (2021). Solid wastes: Alternative materials for cementitious composites production. In *Sustainable Resource Management*, 199–220. Elsevier. https://doi.org/10.1016/B978-0-12-824342-8.00012-2

Das, S. K., Singh, S. K., Mustakim, S., Mishra, J., Das, S. K., & Patel, A. (2020). *Incorporation of Ultrafine Rice Husk Ash (URHA) in Geopolymer Concrete* [Technical report]. ASTM International. https://doi.org/10.13140/RG.2.2.14633.98408

Das, S. K., Tripathi, A. K., Kandi, S. K., Mustakim, S. M., Bhoi, B. and Rajput, P. (2023). Ferrochrome slag: A critical review of its properties, environmental issues and sustainable utilization. *Journal of Environmental Management*, 326(Part A), 116674. https://doi.org/10.1016/j.jenvman.2022.116674

Eba, H., Yonemoto, K. and Suzuki, Y. (2021). Change of state of lime phase and inhibition of hydration reaction by coexisting oxides in steelmaking slag. *ISIJ International*, 61(5), 1594–1602. https://doi.org/10.2355/ISIJINTERNATIONAL.ISIJINT-2020-602

European Committee for Standardization (CEN). (2011). EN 196-5:2011 – Methods of Testing Cement – Part 5: Pozzolanicity Test for Pozzolanic Cement. Brussels.

European Committee for Standardization (CEN). (2013). EN 196-2:2013 – Methods of Testing Cement – Part 2: Chemical Analysis of Cement. Brussels.

European Committee for Standardization (CEN). (2016). EN 196-1:2016 – Methods of Testing Cement – Part 1: Determination of Strength. Brussels.

European Committee for Standardization (CEN). (2016). EN 196-3:2016 – Methods of Testing Cement – Part 3: Determination of Setting Time and Soundness. Brussels.

European Committee for Standardization (CEN). (2018). EN 196-6:2018 – Methods of Testing Cement – Part 6: Determination of Fineness. Brussels.

European Committee for Standardization (CEN). (1999). EN 1015-3: Methods of test for mortar for masonry – Part 3: Determination of consistence of fresh mortar (by flow table). Brussels.

Hewlett, P. C. and Liska, M. (Eds.). (2019). *Lea's Chemistry of Cement and Concrete* (5th ed.). Butterworth-Heinemann, Oxford.

Ho, Q. V. and Huynh, T.-P. (2024). Improving corrosion resistance and prolonging the service life of high-performance concrete structures using fly ash and ground granulated blast-furnace slag. *Periodica Polytechnica Civil Engineering, 68*(2), 669–683. http://dx.doi.org/10.3311/PPci.23572

Holappa, L. E. and Xiao, Y. (2004). Slags in ferroalloys production – Review of present knowledge. *Journal of the Southern African Institute of Mining and Metallurgy*, 104(7), 429–437. https://hdl.handle.net/10520/AJA0038223X_2944

Humad, A. M., Habermehl-Cwirzen, K. and Cwirzen, A. (2019). Effects of fineness and chemical composition of blast furnace slag on properties of alkali-activated binder. *Materials, 12*(20), 3447. http://dx.doi.org/10.3390/ma12203447

Jacob, L. (2024). Ladle furnace slag: Synthesis, properties, and applications. *ChemBioEng Reviews*, 11(1), 60–78. https://doi.org/10.1002/cben.202300024

Karhu, M., Talling, B., Piotrowska, P., Matas Adams, A., Sengottuvelan, A., Huttunen-Saarivirta, E., Boccaccini, A. R. and Lintunen, P. (2020). Ferrochrome slag feasibility as a raw material in refractories: Evaluation of thermo-physical and high-temperature mechanical properties. *Waste and Biomass Valorization*, 11, 7147–7157. https://doi.org/10.1007/s12649-020-01092-4

Kriskova, L., Pontikes, Y., Zhang, F., Cizer, Ö., Jones, P. T., van Balen, K. and Blanpain, B. (2013). Valorisation of stainless steel slags as a hydraulic binder. *Acta Metallurgica Slovaca*, 19(3), 176–183. https://doi.org/10.12776/ams.v19i3.159

Kurdowski, W. (2014). *Cement and Concrete Chemistry.* Springer, Dordrecht. https://doi.org/10.1007/978-94-007-7945-7

Lee, H.-S., Wang, X.-Y., Zhang, L.-N. and Koh, K.-T. (2015). Analysis of the optimum usage of slag for the compressive strength of concrete. *Materials, 8*(3), 1213–1229. http://dx.doi.org/10.3390/ma8031213

Leklou, N. and Das, S. K. (2023). Effect of curing temperatures on hydration, mechanical and microstructural properties of metakaolin-blended cement mortars. *Journal of Thermal Analysis and Calorimetry*, 148(14), 6747–6760. https://doi.org/10.1007/s10973-023-12228-8

Li, Y., Liu, Y., Gong, X., Nie, Z., Cui, S., Wang, Z. and Chen, W. (2016). Environmental impact analysis of blast furnace slag applied to ordinary Portland cement production. *Journal of Cleaner Production, 120,* 221–230. http://dx.doi.org/10.1016/j.jclepro.2015.12.071

Lothenbach, B., Scrivener, K. and Hooton, R. D. (2011). Supplementary cementitious materials. *Cement and Concrete Research, 41*(12), 1244–1256. http://dx.doi.org/10.1016/j.cemconres.2010.12.001

Montañez-Cervantes, M. A., González-Núñez, R., Huirache-Acuña, R. and Castro-Montoya, A. J. (2024). Parametric analysis about the synthesis of metakaolin-based geopolymers. Revista Mexicana de Ingeniería Química, 23(3), 1–15. https://doi.org/10.24275/rmiq/Mat24306

Najm, O., El-Hassan, H. and El-Dieb, A. S. (2021). Ladle slag characteristics and use in mortar and concrete: A comprehensive review. *Journal of Cleaner Production*, 288, 125584. https://doi.org/10.1016/j.jclepro.2020.125584

Nicula, L. M., Manea, D. L., Simedru, D., Cadar, O., Becze, A. and Dragomir, M. L. (2023). The influence of blast furnace slag on cement concrete road by microstructure characterization and assessment of physical-mechanical resistances at 150/480 days. *Materials, 16*(9), 3332. http://dx.doi.org/10.3390/ma16093332

Owaid, H. M., Hamid, R. and Taha, M. R. (2012). A review of sustainable supplementary cementitious materials as an alternative to all-Portland cement mortar and concrete. *Australian Journal of Basic and Applied Sciences, 6*(9), 287–303. Available at: https://www.researchgate.net/publication/285956186.

Puertas, F., Martínez-Ramírez, S., Alonso, S. and Vázquez, T. (2000). Alkali-activated slag mortars: Strength behavior and hydration products. *Cement and Concrete Research, 38*(2), 222–230. http://dx.doi.org/10.1016/S0008-8846(00)00298-2

Ramírez-Arreola, D. E., Aranda-García, F. J., Sedano-de la Rosa, C., Camacho-Vidrio, A. M. and Silva, R. V. (2020). Corrosion behavior of steel reinforcement bars embedded in concrete with sugar cane bagasse ash. Revista Mexicana de Ingeniería Química, 19, sup.1, 469–481. https://doi.org/10.24275/rmiq/Mat1651

Ryu, G. U., Kim, H. J., Yu, H. J. and Pyo, S. (2024). Utilization of steelmaking slag in cement clinker production: A review. *Journal of CO_2 Utilization*, 84, 102842. https://doi.org/10.1016/j.jcou.2024.102842

Schneider, M., Romer, M., Tschudin, M. and Bolio, H. (2011). Sustainable cement production—present and future. *Cement and Concrete Research, 41*(7), 642–650. http://dx.doi.org/10.1016/j.cemconres.2011.03.019

Scrivener, K. L., John, V. M. and Gartner, E. M. (2018). Eco-efficient cements: Potential economically viable solutions for a low-CO_2 cement-based materials industry. *Cement and Concrete Research, 114,* 2–26. http://dx.doi.org/10.1016/j.cemconres.2018.03.015

Scrivener, K., Ouzia, A., Juilland, P. and Mohamed, A. K. (2019). Advances in understanding cement hydration mechanisms. *Cement and Concrete Research*, 124, 105823. https://doi.org/10.1016/j.cemconres.2019.105823

Siddique, R. and Bennacer, R. (2012). Use of iron and steel industry by-product (GGBS) in cement paste and mortar. *Resources, Conservation and Recycling, 69,* 29–34. http://dx.doi.org/10.1016/j.resconrec.2012.09.002

Siddique, R. and Kaur, D. (2012). Properties of concrete containing ground granulated blast furnace slag (GGBFS) at elevated temperatures. *Journal of Advanced Research, 3*(1), 45–51. http://dx.doi.org/10.1016/j.jare.2011.03.004

Singla, R., Kumar, S. and Alex, T. C. (2020). Reactivity alteration of granulated blast furnace slag by mechanical activation for high volume usage in Portland slag cement. *Waste and Biomass Valorization*, 11, 2983–2993. https://doi.org/10.1007/s12649-019-00580-6

Taylor, H. F. W. (1997). *Cement Chemistry* (2nd ed.). Thomas Telford.

Torres-Ochoa, J. A., Osornio-Rubio, N. R., Jiménez-Islas, H., Navarrete-Bolaños, J. L. and Martínez-González, G. M. (2019). Synthesis of a geopolymer and use of response surface methodology to optimize the bond strength to red brick for improving the internal coating in burner kilns. Revista Mexicana de Ingeniería Química, 18(1), 361–373. https://doi.org/10.24275/uam/izt/dcbi/revmexingquim/2019v18n1/TorresO

Thomas, M. (2013). *Supplementary Cementing Materials in Concrete* (1st ed.). CRC Press. https://doi.org/10.1201/b14493

Tole, I., Habermehl-Cwirzen, K. and Cwirzen, A. (2019). Mechanochemical activation of natural clay minerals: An alternative to produce sustainable cementitious binders – review. *Mineralogy and Petrology, 113,* 449–462. http://dx.doi.org/10.1007/s00710-019-00666-y

Tripathi, A. K., Das, S. K., Mustakim, S. M., Kandi, S. K. and Rajput, P. (2025). Integrated management of ferrochrome slag: Metal recovery, Cr(VI) stabilization, and sustainable reuse in construction materials. *Journal of Environmental Management*, 390, 126268. https://doi.org/10.1016/j.jenvman.2025.126268

Vlcek, J., Švrčinová, R., Burda, J., Topinková, M., Klárová, M., Ovcačíková, H., Jančar, D. and Velíčka, M. (2016). Hydraulic properties of ladle slags. *Metalurgija*, 55(3), 399–402. https://hrcak.srce.hr/index.php/153630

Yan, J., Wu, S., Yang, C., Zenggang, Z. and Xie, J. (2022). Influencing mechanisms of RO phase on the cementitious properties of steel slag powder. *Construction and Building Materials*, 350, 128926. https://doi.org/10.1016/j.conbuildmat.2022.128926

Zhang, Z., Cao, P., Wang, Y., Zhao, X. and Liu, J. (2024). Effect of Fe and Mn on the hydration activity of f-CaO in steel slag. *Construction and Building Materials*, 421, 135719. https://doi.org/10.1016/j.conbuildmat.2024.135719

Zhao, J., Yan, P. and Wang, D. (2017). Research on mineral characteristics of converter steel slag and its comprehensive utilization of internal and external recycle. *Journal of Cleaner Production*, 156, 50–61. https://doi.org/10.1016/j.jclepro.2017.04.029

Zhuang, S. and Wang, Q. (2021). Inhibition mechanisms of steel slag on the early-age hydration of cement. *Cement and Concrete Research*, 140, 106283. https://doi.org/10.1016/j.cemconres.2020.106283